Effect of Additional Unpaired Bases on the Stability of Three-Way DNA Junctions Studied by Fluorescence Techniques†

Frank Stühmeier,‡ David M. J. Lilley,§ and Robert M. Clegg*,‡

Max-Planck-Institut für biophysikalische Chemie, Abteilung Molekulare Biologie, Am Fassberg 11, D-37077 Göttingen, Germany, and Cancer Research Campaign Nucleic Acid Structure Research Group, Department of Biochemistry, The University, Dundee DD1 4HN, United Kingdom

Received February 3, 1997; Revised Manuscript Received July 11, 1997⊗

ABSTRACT: Fluorescence melting experiments were carried out to determine the relative stability of three-way DNA junctions with and without extrahelical adenine nucleotides in one strand at the branch point of the junction (i.e., A_n bulges where $n = 0$, 1, 2, and 3). The oligonucleotides were labeled with chromophores at the 5′ ends of the strands. The progress of the thermal denaturation was followed by monitoring the fluorescence intensities and anisotropies of the dyes and the fluorescence resonance energy transfer between the two dyes. The results of the thermal denaturation experiments are interpreted and discussed in terms of either two-state thermodynamic models or statistical models for the thermal denaturation. The junctions all melt at the same temperature (at equal concentrations) within the error of the T_m determination, regardless of the presence, or absence, of the bulge. It is suggested that the denaturation of the helical arms begins primarily at the free ends of the helical arms and proceeds toward the branch point. The junctions, all which have 10 base pairs in each arm, possess thermal denaturation characteristics similar to duplexes with 20 arms. This leads to the proposition that for these junctions an important molecular parameter that controls the stability of the junctions is the number of base pairs between neighboring arms. The melting profiles obtained by monitoring the tetramethylrhodamine fluorescence are found to depend strongly on the nucleotide sequence in the single-stranded region.

Branched molecular structures, such as the four- and three-way DNA junctions and bulged duplexes have been proposed to play an important role as possible intermediates in molecular rearrangements, repair, and recombination. An introduction to the literature of branched junctions, and three-way junctions in particular, can be found in the previous paper (Stühmeier et al., 1997); in that paper, we determined the global structure of a three-way junction with and without additional bases at the branch point using fluorescence resonance energy transfer (FRET).[1]

The stability of the total duplex structure of complementary DNA strands is manifested in thermal denaturation experiments. The effect of a branch point on the thermodynamic stability and dynamics of branched nucleic acid molecules has been studied by several groups in the last few years (Husler & Klump, 1994, 1995; Ladbury et al., 1994; Leontis et al., 1991; Zhong et al., 1993, 1994). It has been reported that the presence of the unpaired nucleotides in one strand at the branch point (this constitutes a bulge) both stabilizes (Leontis et al., 1991; Zhong et al., 1994) or destabilizes (Ladbury et al., 1994) the overall stability of the branched three-way junctions. Some of these data have come from calorimetric experiments which can furnish the total enthalpy (ΔH) and the total entropy (ΔS) for the overall conversion from the fully base-paired state to the fully single-stranded state. Direct structural information is lacking in calorimetric experiments, although molecular models for the progress of the reaction can be compared to the data from differential scanning calorimetry (Marky & Breslauer, 1987). The sequences of the bulges for which the thermal stability of the three-way junctions has been more systematically studied are A1-3, A5, C2 (Welch et al., 1995); T1-4 and A1-4 (Zhong et al., 1994); T2 (Overmars et al., 1996); A2 (Ladbury et al., 1994); and A2-3 (Leontis et al., 1991).

Electrophoresis studies (Leontis et al., 1991) suggested that three-way junctions with short arms might be stabilized by the inclusion of extra unpaired bases, although this conclusion is not in accord with more refined thermodynamic studies on similar molecules with somewhat longer arms to stabilize the duplex structure (Ladbury et al., 1994). Zhong et al. (1994) reported only a very marginal stabilization at 20 °C of three-way junctions ($\Delta\Delta G \approx 1$ kcal mol^{-1}) with the inclusion of two bulged nucleotides, although the $\Delta\Delta H$ of hybridization was increased by 4−5 kcal mol^{-1}. In several studies, the presence of three or more unpaired nucleotides leads to a destabilization compared to the junction without bulged nucleotides (Leontis et al., 1991; Welch et al., 1993, 1995; Zhong & Kallenbach, 1993).

In this paper, we have used fluorescence methods to follow the thermally induced denaturation of a series of 3H and $3HS_n$ molecules[2] ($n = 1-3$) with which we have previously carried out electrophoresis (Welch et al., 1993) and fluorescence (Stühmeier et al., 1997) studies of their solution structures. Fluorescence serves as a convenient method for

† D.M.J.L. thanks the CRC for financial support, and R.M.C. and D.M.J.L. thank the British Council-DAAD for a travel grant. F.S. and R.M.C. thank the Deutsche Forschungsgemeinschaft for financial support: DFG-Project Nr. II B 2 C1 84/2-2.

* Author to whom correspondence should be addressed.

‡ Max-Planck-Institut für biophysikalische Chemie.

§ The University.

⊗ Abstract published in *Advance ACS Abstracts,* September 15, 1997.

[1] Abbreviations: FRET, fluorescence resonance energy transfer; TMRh, tetramethylrhodamine; NMR, nuclear magnetic resonance; TB, Tris borate buffer.

S0006-2960(97)00245-6 CCC: $14.00

monitoring the influence of bulges on the progress of the thermal denaturation of the three-way junction and to determine the extent of thermodynamic coupling between the helical arms that contributes to their stabilities. In the previous paper in this issue (Stühmeier et al., 1997), we have detected distinct structural differences between three-way junctions with and without bulges at the branch point. We have proposed in that study that stacking between the ends of two of the helical arms at the junction could be responsible for an approximate coaxial arrangement of these two arms in the junctions with bulges. In this paper, we report on thermal denaturation studies of these junction molecules in order to inquire whether the melting profiles of the molecules with and without bulges can detect stabilizing or destabilizing interactions at the branch point of the three-way junctions. Large differences in the tetramethylrhodamine (TMRh) fluorescence properties of the different single-stranded sequences are found in the melting profiles. This effect is interpreted in terms of sequence effects on the fluorescence intensity of TMRh attached to DNA.

MATERIALS AND METHODS

Preparation and Characterization of the Oligonucleotides. The labeled oligonucleotides and all the three-way junction molecules used in the thermal denaturation studies are identical to those molecules discussed in the previous paper (Stühmeier et al., 1997). That paper should be consulted for the preparation and the characterizations of the oligonucleotides. For reference we list the sequences of the single strands that are used to construct the junctions, which simultaneously identifies our notation of the three strands (h, r, and x): h-strand, 5′ CCT AGC AGC GAG AGC GGT GG 3′; x-strand, 5′ CCA GTT GAG ACG CTG CTA GG 3′; r-strand s0, 5′ CCA CCG CTC T TC TCA ACT GG 3′; r-strand s1, 5′ CCA CCG CTC TA TC TCA ACT GG 3′; r-strand s2, 5′ CCA CCG CTC TAA TC TCA ACT GG 3′; r-strand s3, 5′ CCA CCG CTC TAAATC TCA ACT GG 3′.

Fluorescence Measurements. The fluorescence measurements were carried out and analyzed exactly as described in the previous paper in this issue (Stühmeier et al., 1997), which should be consulted for details. The FRET efficiencies were determined by measuring the intensity of the sensitized emission of the acceptor normalized to the fluorescence of the acceptor alone (Clegg, 1992). The spectral dispersion of the fluorescence intensities of the emission spectra $F(\lambda_{em}, 490)$ (excited at 490 nm, where both D and A absorb) are fitted to the weighted sum of two spectra components: (1) a standard spectrum of a three-way junction labeled only with donor $F^D(\lambda_{em}, 490)$ and (2) the fluorescence spectrum of the sample $F(\lambda_{em}, 560)$ excited at 560 nm, where only TMRh absorbs.

$$F(\lambda_{em}, 490) = aF^D(\lambda_{em}, 490) + (\text{ratio})_A F(\lambda_{em}, 560) \quad (1)$$

a and $(\text{ratio})_A$ are the weighting factors for the two spectral components that are fitted in the regression analysis. The coefficient $(\text{ratio})_A$ can be shown to be equal to

$$(\text{ratio})_A = \frac{F(\lambda_{em}, 490) - aF^D(\lambda_{em}, 490)}{F(\lambda_{em}, 560)} = Ed^+\frac{\epsilon^D(490)}{\epsilon^A(560)} + \frac{\epsilon^A(490)}{\epsilon^A(560)} \quad (2)$$

$(\text{ratio})_A$ is linearly dependent on the efficiency of energy transfer E. It normalizes the measured sensitized FRET signal for the concentration and for the apparent quantum yield[3] of the acceptor and accounts for errors in the percentage of acceptor labeling. d^+ is the fraction of labeling with donor molecules. ϵ^D and ϵ^A are the molar absorption coefficients of D and A at a given wavelength. $\epsilon^D(490)/\epsilon^A(560)$ and $\epsilon^A(490)/\epsilon^A(560)$ were determined from the absorbance spectra of the doubly labeled molecules and the excitation spectra of singly TMRh labeled molecules.

Fluorescence Melting Curves. The thermal denaturation of the three-way junctions was followed by measuring several fluorescence parameters (relative apparent quantum yields, anisotropy, and the FRET values calculated from the pertinent spectra at each temperature). The DNA samples were first dialyzed into 90 mM Tris borate (pH 8.3), 100 mM NaCl, and 0.5 mM EDTA and finally dialyzed twice into the same buffer without EDTA. The samples were degassed for 10 min at room temperature, covered with degassed paraffin-oil in the cuvette, and then stored for 3 days at 4 °C before doing the measurements. The temperature was increased in steps of 2−4 °C. The temperature was measured by inserting a microthermistor into a cuvette filled with 50% ethylene glycol in a second identical water-jacketed cuvette holder. The fluorescence measurements began 10 min after the desired temperature was reached. No kinetic changes were observed at any time during the denaturation experiments reported here. All samples used for the melting curves had the same optical density of DNA (OD(260) $\approx 0.05 \pm 0.002$) to avoid artifacts from concentration effects.

Spectroscopic Measurements for Following the Progress of Melting. The following special attributes of the three different spectroscopic methods used for following the progress of the thermal denaturation are based on our earlier studies with similar molecules (Clegg et al., 1994; Vámosi et al., 1996) and on previous measurements in our laboratory (C. Gohlke et al., unpublished work; G. Vámosi et al., unpublished work).

(1) Direct Measurement of the Relative Apparent Quantum Yield of the Energy Donor Fluorescein. The change of the fluorescence intensity of fluorescein is a superposition of the change of the FRET efficiency during the melting process

[2] The notation of branched nucleic acid structures proposed by Lilley et al. (1995) will be used in the text. For the three way junctions $3HS_n$ means three helical arms meeting at a branch point and a single stranded loop of n nucleotides on one of the strands. 3H refers to a three-way junction without a bulge (only three helices).

[3] Throughout the text we will use the term "apparent quantum yield" when referring to relative measured fluorescence intensities of samples which are excited with light of the same intensity. The true quantum yield of a fluorescent molecular species is a measure of the number of quanta emitted relative to the number of photons absorbed and is a term which can only be used when referring to one single fluorescent species; however, if there are multiple fluorescing species in solution, which may even interconvert, we can only measure parameters related to an apparent quantum yield of the mixture in a steady-state fluorescence measurement. In addition, it could be that samples being compared have different absorption coefficients, and then, even if the samples are composed of single chromophore species, the true ratio of their fluorescence intensities is not the ratio of their quantum yields.

and the change of the apparent quantum yield and the absorption coefficient of the dye during the double-stranded (ds) to single-stranded (ss) transition. For singly labeled molecules, the apparent fluorescence quantum yield of fluorescein (in the absence of TMRh) is higher in the single- than in the double-stranded form. Changes in the absorption spectrum of fluorescein are minimal. For the doubly labeled $3HS_n$ molecules, fluorescein also serves as an energy donor to TMRh. This additional pathway for deactivation from the excited state means that the apparent quantum yield of fluorescein depends not only on its local environment but also on the distance between the fluorescein and the TMRh chromophores.

(2) Direct Measurement of the Relative Apparent Quantum Yield of TMRh. TMRh can be excited separately from fluorescein, and there is no energy transfer from TMRh to fluorescein. The helix−coil transition can be monitored by measuring the fluorescence intensity and anisotropy of TMRh. For some of the sequences, the changes in the TMRh fluorescence anisotropy during the melting process are not very large (see Results and below) and the analysis of these TMRh fluorescence anisotropy melting curves are accordingly not as accurate. The changes in the apparent quantum yield and in the anisotropy of TMRh during the melting process reflect mainly changes in the interaction between the chromophores and DNA when passing from the double- to the single-stranded state and are sensitive to partially melted molecular species. The physical reason for the temperature dependence of the fluorescence parameters of TMRh−DNA complexes has been recently reported (Vámosi et al., 1996).

(3) Temperature Dependence of the FRET Efficiency. The FRET efficiency can be determined conveniently at different temperatures by determining the normalized sensitized emission of the acceptor dye, i.e., $(\text{ratio})_A$ (eq 2). The FRET efficiency drops to zero upon dissociation of the two complementary DNA strands labeled with donor and acceptor, respectively. The fluorescence values in the denominator of the equation for $(\text{ratio})_A$ normalize the fluorescence values in the numerator for the number of molecules in the measured volume. If there is a single molecular species of 100% labeled molecules in solution, $(\text{ratio})_A$ (and similarly TMRh anisotropy) is corrected properly for the concentration of labeled molecules by the denominator in eq 2; however, in the transition region, both double-stranded (ds) and single-stranded (ss) molecular species with very different fluorescence characteristics are simultaneously present, and their relative concentrations change rapidly in the transition region. The disparate temperature variations of the fluorescence properties of the double- and single-stranded molecular species in the scaling denominator of $(\text{ratio})_A$ (see eq 2) lead to nonlinear alterations that must be taken into account during the fitting of $(\text{ratio})_A$ melting curves. If this effect is not taken into account when extracting the extent-of-melting curves from the $(\text{ratio})_A$ melting curves, the extent-of-melting curves can be considerably offset, resulting in erroneous values of T_m that do not correspond, even approximately, with 50% strand dissociation. Therefore, during the fitting procedure of the $(\text{ratio})_A$ curves the difference between the ds- and ss-fluorescence intensities is included in the functional analysis of the extent-of-melting curve (details of this analysis are given in Vámosi et al., manuscript in preparation).

Baseline Extraction. One of the main difficulties in quantifying optically detected melting curves is determining the effect of the baselines due to temperature-dependent spectroscopic changes within the transition region of the purely double-stranded or purely single-stranded forms of the DNA. This has been discussed in the literature in relation to absorption melting curves. It is often difficult to separate the contribution of the baselines to the signal in the transition region from the spectroscopic changes originating from the actual molecular transition, especially if these baselines are strongly sloping. We have taken two approaches to extract baselines from the fluorescence melting data for analyzing the denaturation experiments.

(1) The most common method (Marky & Breslauer, 1987) is to estimate straight lines from the data points that are exclusively on either side of the melting transition. The difference between each data point and the straight line for the helix is then normalized by dividing it by the difference between the two straight lines at each corresponding temperature; this yields an extent-of-melting curve with values from 0 to 1. This simple analysis assumes that the spectroscopic signals of the pure helix and pure coil states vary approximately linearly with temperature in the small temperature range of interest within the transition region. Sufficient data must also exist on both sides of the transition, and fully outside the transition, so that a reliable linear fit can be made to the baselines. For the relative fluorescence intensity of the fluorescein and the $(\text{ratio})_A$ values, the baselines were fitted with straight lines from 4 to 20 °C (lower baseline) and from about 50 to about 70 °C (upper baseline). For the relative fluorescence intensity of the TMRh, the lower baseline was fitted with a straight line from 4 to about 20 °C, and the upper baselines were fitted from 48 to 70 °C for the $3HS_n$(hR) and $3HS_n$(rR) molecules and from 48 to 58 °C for the $3HS_n$(xR) molecules. This was necessary for the analysis of the TMRh curves because the spectroscopic parameters of the acceptor in the single-stranded region depend strongly on the sequence composition of the oligonucleotide. This simple method for analyzing the data was sufficient for most of the molecules and agreed with the following more complex baseline correction.

(2) In the second method, the baselines are fitted simultaneously with the thermodynamic model. If the temperature dependence of the spectroscopic signals of the pure helix and pure coil states are known, these data can be used directly in the fitting procedure. In this paper, when fitting with this method, we assume (as in the first method) that the true baselines can be approximated by linear curves. The baselines are then determined by fitting all the data directly to a functional representation of a two-state bimolecular reaction (which displays a fluorescence change during the progress of the reaction) together with the two linear processes on either side of the transition. The extracted extent-of-melting curves are still obtained by removing the linear baselines, as in method 1; however, the functional dependence of the helix-to-coil transition has approximately been taken into account simultaneously with the determination of the baselines. The transition need not be two-state for this procedure to work well, and the effect of the shape of the transition curve is minimal, even for non-two-state transitions, as shown by simulations. If the transition is really a two-state process, the thermodynamic parameters governing the transition can be taken directly from the fit. The T_ms

and the extent-of-melting curves were often almost identical using both methods. If there was a significant difference in using the two methods, the second method was preferred.

The Two-State Reaction Models Used for Analyzing the Melting Curves. The two-state reaction of the $3HS_n$ duplex molecules from the double-stranded state to the single-stranded state was analyzed according to two reaction models. (1) The hybridization process was assumed to be a trimolecular two-state reaction of a 30 bp duplex DNA molecule, where the hybridization of the single strands for forming a duplex molecule is represented by

$$ss_1 + ss_2 + ss_3 \leftrightarrow ds, \quad \text{with } K_{diss} = [ss_1][ss_2][ss_3]/[ds] \tag{3A}$$

(2) The second model assumes the controlling association step to take place as a bimolecular two-state reaction of a 10 bp, 20 bp, or a 30 bp duplex DNA molecule.

$$ss_1 + ss_2 \leftrightarrow ds, \quad \text{with } K_{diss} = [ss_1][ss_2]/[ds] \tag{3B}$$

The ΔH and T_m values from the two-state analyses were derived from the extent-of-melting curves (see Appendix, eqs A7 and A8). When the shape of the melting curves for the TMRh labeled samples could be well simulated globally by a two-state reaction (eqs 3A or 3B), the ΔH and ΔS values for the transition were determined from a nonlinear regression analysis directly to the extent-of-melting curve (eq A7), or by the second method of baseline extraction (see above and eq A8). Whenever the global shape of the curve showed deviations from that of a pure two-state model, the thermodynamic analysis for determining ΔH and ΔS was restricted to the center of the transition (about the half-way point). This was easily done by fitting a plot of $\ln(\alpha^n/(1-\alpha))$ vs $1/T$ (where $n = 2$ and 3, and α is the extent-of-melting) to a linear function in the melting region (this is in the temperature range from 32 to 44 °C for all the samples). For the fluorescein melting curves, the two-state analysis according to eq 3B fit the data well throughout the whole melting transition. The two-state ΔH and ΔS values are apparent parameters, defined operationally by this fitting analysis.

Simulation of Melting Curves with the Statistical Zipper Model. In the statistical zipper model, each base pair of an oligomer can exist individually in a double-stranded (helical) or single-stranded (coil) state. A simple two-stranded duplex helix can melt from both ends independently and concurrently. No internal base pairs of a double-stranded stretch of helix are allowed to melt; in the model, stepwise melting of the base pairs is allowed only from the outside ends of an oligomer. This assumption is made because configurational states with internal loops are highly improbable due to the entropy penalty accompanying the formation of internal loops (Poland & Scheraga, 1970).[4]

A statistical weight is assigned to each possible overall molecular conformation of the oligomer (i.e., all permutations and combinations of helical and coil states of all the individual base pairs) consistent with the constraint that the oligomers melt from the ends. The enthalpy and entropy change per base pair ΔH_i/bp and ΔS_i/bp due to the melting reaction of each ith base pair can be assigned individually. In general, ΔH_i/bp and ΔS_i/bp depends upon i, i.e., on the local sequence and context of the ith position of the base pair, but in this study these parameters are assumed to be equal for all base pairs, and these average values are designated as ΔH/bp and ΔS/bp. Unless otherwise specified, the value for ΔS_i/bp is always assumed to be 0.024 kcal (mol bp)$^{-1}$ K^{-1}. This is the value often assumed in the literature when analyzing curves for smaller oligonucleotides with the two-state model (Breslauer et al., 1986).

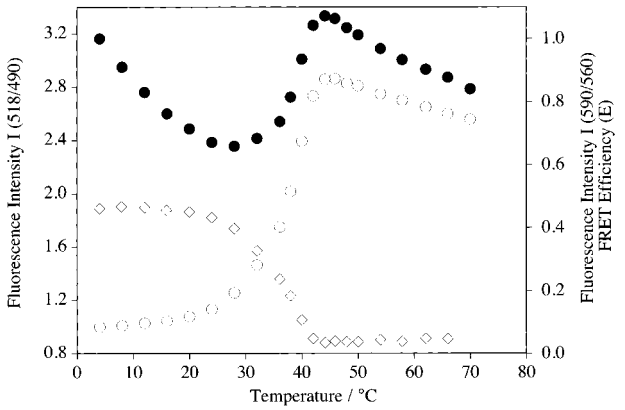

FIGURE 1: The thermal denaturation of the sample $3HS_3$(hRrF) monitored with the fluorescence intensities of fluorescein (open circles) and TMRh (filled circles) and from the changes of the FRET efficiency E values (open diamonds). The helix−coil transition starts at ~30 °C and is finished at ~42 °C; the melting curves are analyzed as described in the text.

The fluorescence properties of the dyes (e.g., apparent quantum yield and the anisotropy) are affected mostly by changes in the hybridization state of the nucleotides near the site of dye attachment (Vámosi et al., 1996). In general, it is not known how many, or which, nucleotides at the helix end (or end of the labeled single strands) directly influence the fluorescence of the conjugated dyes, how much each base contributes to the fluorescence change, and to which extent the actual nucleotide sequence plays a role. At the moment, we treat this problem empirically for each individual case. Details of the statistical analysis are given in the Appendix.

RESULTS

Melting of the Three-Way DNA Junction at 100 mM NaCl Monitored with Different Fluorescence Spectroscopic Parameters. We examined the thermal stability of the $3HS_n$ molecules over a temperature range from 4 to 70 °C. The progress of the temperature-induced helix−coil transition was followed by several different spectroscopic measurements (Figure 1): (1) the change in the relative apparent fluorescence quantum yield of fluorescein, (2) the change in the relative apparent quantum yield of TMRh, and (3) the change in the $(\text{ratio})_A$ values. The $(\text{ratio})_A$ value of a single doubly labeled molecular species is linearly related to the efficiency

[4] In support of this assumption, as we show later in this paper, we also have no FRET evidence for an opening of a "folded, stacked" configuration prior to the main melting transition in the thermal denaturation curves of the $3HS_n$ molecules with $n = 1$, 2, and 3 (see Stühmeier et al., 1997); if a stacked configuration at the branch point would be unfolded prior to the main transition, we would expect the overall relative orientation of the arms to change drastically, thereby affecting the FRET efficiency. In addition, statistical mechanical simulations of the melting process of our $3HS_n$ molecules (where the dye labeling is on the outside ends of the arms) indicate that the form of the melting curves cannot be represented well if the molecules open up from the inside (i.e., if the melting starts from a position in the molecule far removed from the location of the dye).

of energy transfer (see eq 2), and the efficiency of FRET is zero upon dissociation of the DNA structure into the single strands. The results of these different spectroscopic measurements can be summarized as follows.

(1) The apparent fluorescence quantum yield of fluorescein (excitation at 490 nm and emission at 518 nm) is constant within 10% in the temperature range from 4 to 20 °C. It increases strongly from 30 to 45 °C and decreases slightly from 45 to 70 °C (Figure 1). This large change during the helix−coil transition is mainly caused by the increase of the apparent quantum yield of the dye and partially by the decrease of the FRET efficiency; it cannot be explained only by changes in the dye's absorption coefficient, which plays only a minor role (Vámosi et al., 1996).

(2) The fluorescence intensity of TMRh (excitation at 560 nm and emission at 590 nm) decreases strongly from 4 to 25 °C, increases from 30 to 45 °C, and finally decreases from 45 to 70 °C (Figures 1 and 3). TMRh can be excited separately without exciting fluorescein, so that the change in the fluorescence intensity of TMRh is not influenced by changes of the FRET efficiency. The melting process can also be monitored by the changes of the fluorescence anisotropy of TMRh (Figure 4).

(3) The value of the normalized sensitized emission of the acceptor, i.e., $(\text{ratio})_A$, depends on the structure of the DNA molecule and on the small temperature induced changes in the ratios of the absorption coefficients (eq 2) during the process of melting. The absorption changes are very small and can be taken into account; the correction does not significantly affect the results of the denaturation experiment (Vámosi et al., 1996). The $(\text{ratio})_A$ values remain approximately constant up to a temperature of ~25 °C and strongly decrease from 30 to 40 °C. The $(\text{ratio})_A$ value in the temperature region where the duplex is completely melted is not zero, but corresponds to the ratio of TMRh fluorescence excited at 490 and 560 nm (see eq 2); this ratio increases slightly with temperature due to the temperature dependence of the relative absorption coefficients of TMRh excited at these different wavelengths (Figure 1).

Quantitative Analysis of the Melting Curves. The melting curves were analyzed in two ways: (1) by assuming that the DNA molecules pass from the ds state to the ss state in one reaction step (two-state process) and (2) by a statistical mechanical simulation within the constraints of a zipper model.

Results of the Two-State Analysis. The T_m of the 3H and $3HS_n$ molecules ($n = 1-3$), determined from the different fluorescence spectroscopic parameters, is not influenced significantly by the number of nucleotides in the bulge at the point of branch exchange or by the spectroscopic parameter used to follow the melting process (Table 1). The two-state analyses lead to T_m values of 38 (±0.5) °C determined from the relative fluorescence intensities of the acceptor molecules and from the "corrected" analysis of the $(\text{ratio})_A$ values (see Materials and Methods); the error refers to the consistency of the T_m values, not to a statistical error. Depending on where the baselines are positioned, the T_m of the donor melting curves are either 38 (±0.5) °C, or 38.5 (±0.5) °C; however, the fitted T_m values within a series of similarly labeled molecules employing similar baseline determinations are within ±0.5 °C.

Within the two-state assumption, the ΔH values given in Table 1 were determined for the melting curves derived from the fluorescence intensities of fluorescein and TMRh by analyzing the slope of the ln K vs $1/T$ plot (where K is defined in terms of α, see the text following eqs 3A and

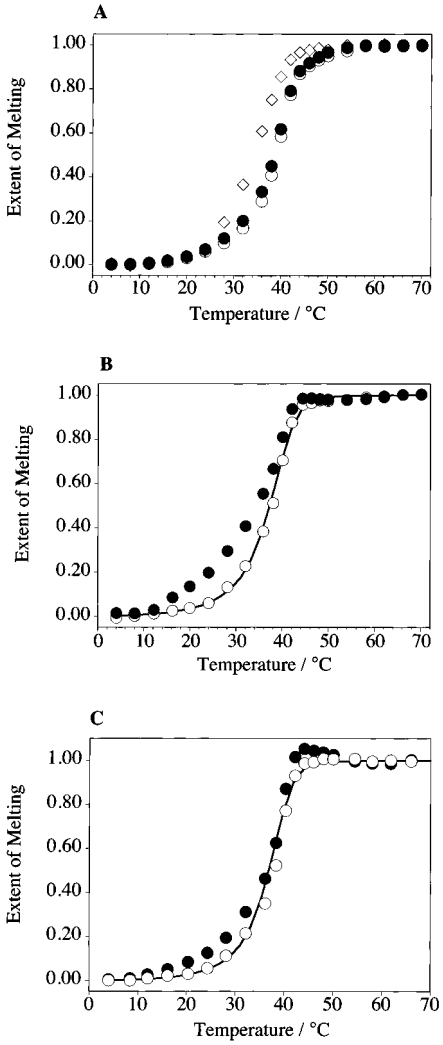

FIGURE 2: Extent-of-melting curves of different $3HS_n$ vectors calculated from different fluorescence properties. (A) Extent-of-melting of the $3HS_1$(hFrR) vector: the curves are calculated from the different fluorescence parameters according to the following notation: open diamonds = FRET; open circles = fluorescein fluorescence intensity; filled circles = TMRh fluorescence intensity. Note that the *apparent* T_m of the FRET melting curve is 3−4 °C lower than for the fluorescence intensity melting curves and that the two melting curves derived from the fluorescence intensities are essentially identical. This is true for all the vectors where the h-strand is labeled with TMRh. The "corrected" FRET extent-of-melting curves (not shown) essentially overlap the fluorescence intensity curves; that is, the correction raises the T_m. (B) Extent-of-melting of the $3HS_2$(hRrF) vector: the filled and open circles are derived from the TMRh and fluorescein intensity data. The smooth line is a fit using the statistical zipper model to the fluorescein intensity extent-of-melting curve. The deviation of the TMRh melting curve at lower temperatures is discussed in the text in terms of possible interactions of TMRh with the thymine at position 3 of the h-strand. (C) Extent-of-melting of the $3HS_3$(rFxR) vector: the open and filled circles are derived from the fluorescein and TMRh intensity data. The smooth line is a fit using the statistical zipper model to the fluorescein intensity extent-of-melting curve. In the text, it is discussed that the deviations of the TMRh melting curve from the fluorescein melting curve may be related to an interaction of the TMRh with the thymines at the 4- and 6-positions on the x-strand. The deviations at lower temperatures is not as pronounced as when TMRh is attached to the h-strand, and the hump seen at the high end of the helix−coil transition is only pronounced when TMRh is attached to the x-strand.

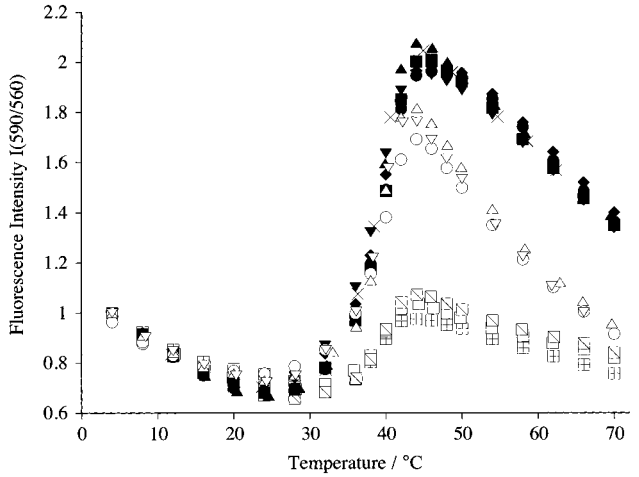

FIGURE 3: The thermal denaturation of the $3HS_n$ junctions monitored by the fluorescence intensity of TMRh [*I* (590/560)]. In each curve, the fluorescence intensity is normalized by the value at 4 °C. From 4 to 12 °C, the fluorescence spectroscopic parameters are very similar for all the molecules. The samples can be divided into three groups: the first group (TMRh at the r arm, upper curves above T_m) has a high fluorescence intensity at higher temperatures; the second group (TMRh at the x arm, middle curves above the T_m) has a considerably lower intensity at higher temperatures; the third group (TMRh at the h arm, lower curves above the T_m) the fluorescence is highly quenched even at relative low temperatures. The melting curves of each group are almost indistinguishable in this plot, so the different three-way molecules are not identified.

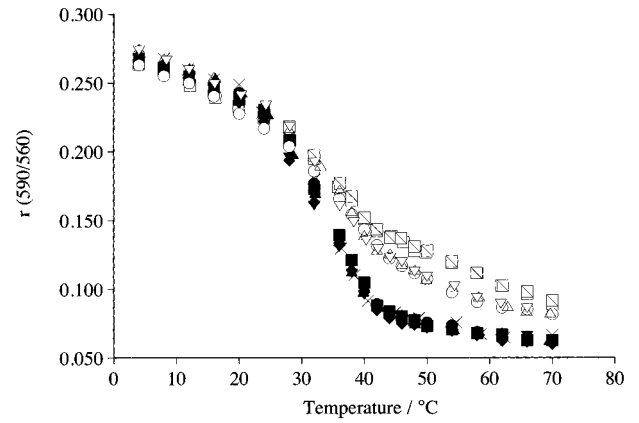

FIGURE 4: Thermal denaturation of the $3HS_n$ molecules monitored by the fluorescence anisotropy, *r* (590/560). The symbols identifying the different molecules correspond exactly to those in Figure 3. The hR and xR samples have a higher anisotropy than the rR samples above the T_m, which is consistent with the proposed differences in the quenching of the fluorescence in the single-stranded region, i.e., the mean fluorescence lifetime is lower for the higher degree of quenching, leading to a higher anisotropy. The highly quenched hR samples have a significantly higher anisotropy at temperatures above the T_m than the xR samples which are not so strongly quenched.

3B) only in the center of the transition (from 36 to 46 °C). The average total ΔH and ΔS for the entire structure of the molecules resulting from the two-state analyses are 128 ± 20 kcal mol^{-1} and 0.38 ± 0.07 kcal (mol K)$^{-1}$, assuming a bimolecular reaction, and 153 ± 30 kcal mol^{-1} and 0.44 ± 0.08 kcal (mol K)$^{-1}$, assuming a trimolecular reaction. If it is assumed that the structure comprises 30 base pairs (i.e., the entire three-way structure) and that the hybridization takes place in a single trimolecular association reaction step, the two-state analysis leads to ΔH values of 5.1 (±1) kcal (mol bp)$^{-1}$ for all three-way junction samples regardless of the spectroscopic parameter used in the analysis (Table 1). If it is assumed that the reaction is bimolecular and that the independent two-state melting structural region constitutes only 10 base pairs, the calculated ΔH per base pair is 12.8 ± 2.5 kcal (mol bp)$^{-1}$. If a two-state bimolecular melting process is assumed for a duplex of 20 base pairs, the ΔH per base pair is 6.4 ± 1.3 kcal (mol bp)$^{-1}$ (see Table 1).

Table 1: ΔH^a and T_m Values of Two-State Fits

parameter	ΔH 30 bp tri	ΔH 10 bp bi	ΔH 20 bp bi
$(\text{ratio})_A$			7.0 ± 0.7
I(518/490)	5.3 ± 0.9	13.1 ± 2.5	6.6 ± 1.5
I(590/560)	4.9 ± 0.8	12.5 ± 2.0	6.3 ± 1.0

parameter	T_m (two-state)
I(590/560) TMRh (h-strand)	38.0 ± 0.6
I(590/560) TMRh (r-strand)	38.3 ± 0.4
I(590/560) TMRh (x-strand)	38.5 ± 0.3
I(518/490)	38.5 ± 0.5
$(\text{ratio})_A$	38.6 ± 0.4

[a] ΔH values of the different two-state fits of the fluorescence melting curves. ΔH 30 bp tri is the ΔH value determined by assuming a trimolecular two-state dissociation reaction of the whole molecule, while the other ΔH values have been determined assuming a bimolecular two-state reaction for 10 or 20 base pairs. [b] T_m values as determined from the two-state fits for the different spectroscopic parameters which have been used to follow the helix−coil transition of the three-way DNA junctions. The melting temperatures are essentially identical; for all the molecules regardless of the spectroscopic parameter used for their determination. The T_m values for the $(\text{ratio})_A$ data has been derived by calculating the extent-of-melting curves are described in the Material and Methods.

The ΔH and ΔS values were also determined from the corrected analysis of the $(\text{ratio})_A$ melting curve. The average total ΔH and ΔS values are 140 ± 14 kcal mol^{-1} and 0.42 ± 0.05 kcal (mol K)$^{-1}$, assuming a bimolecular reaction (Table 1).

Results of the Statistical Zipper Analysis. An example of simulating the extent-of-melting curves according to the statistical zipper model is shown in Figure 2. The simulations were carried out using a variety of molecular and thermodynamic parameters; the variance between the data and the calculated curve was minimized. The extent-of-melting curves calculated from the TMRh fluorescence signals are very similar for all the samples with and without bulges (the same is true of the fluorescein signals). Except for a few experiments, the curves can be represented well globally by a 20 bp duplex with an average ΔH/bp = 7.7 ± 0.5 kcal (mol bp)$^{-1}$ and an average ΔS/bp = 0.024 kcal (mol bp)$^{-1}$ K^{-1}. This result indicates that the cooperative unit of melting in these branched molecules is about 20 base pairs. In several cases, when the two-state 20 bp duplex fits deviate markedly from the data, the deviations are no longer present in the statistical analysis. If it is assumed that the three-way junction molecules melt like 10 bp duplexes (i.e., the length of the arms), the average ΔH/bp and ΔS/bp needed to fit the data with the statistical model [ΔH = 10−11 kcal (mol bp)$^{-1}$ and ΔS = 0.032−0.035 kcal (mol bp)$^{-1}$] are greater than the average values reported in the literature (Breslauer et al., 1986); the requirement of such high ΔH and ΔS values to fit the data is evidence against the proposition that the arms melt independently as 10 bp duplex.

Spectroscopic Characteristics of Single-Stranded TMRh Labeled Oligonucleotides at Higher Temperatures. If we normalize the fluorescence intensity of TMRh to its intensity at 4 °C [we have shown in the previous paper in this issue

(Stühmeier et al., 1997) that the apparent measured fluorescence quantum yield of TMRh at this temperature is essentially identical regardless of which of the arms is labeled], the normalized curves show significant differences at temperatures above the T_m (Figure 3) and the data can be separated into three groups. The fluorescence intensity of the $3HS_n$ (rR) molecules (TMRh on the r-strand) at the end of the melting transition (at about 42 to 44 °C) is double the intensity at 4 °C (Figure 3, upper values), whereas the $3HS_n$ (hR) molecules are quenched significantly more in the single-stranded state (Figure 3) compared to the $3HS_n$ (rR) molecules. The $3HS_n$ (xR) molecules show first an increase in the relative fluorescence intensity comparable to those of rR samples [from I (560/590) = 1.0 at 4 °C to I (560/590) = 1.8 at about 42 °C]. At higher temperatures (from 44 to 70 °C), the relative fluorescence intensities of the xR samples gradually decrease to about 0.8, which is approximately the same as the hR samples. Compared to the rR samples, the extent-of-melting curves for the hR samples from the TMRh fluorescence intensity measurements show an apparent premelting transition at low temperatures (10−20 °C), whereas the xR samples display a slight hump at the higher end of the transition region (Figure 2C). The latter is a result of the pronounced peak of the fluorescence change above the T_m that is especially apparent in the melting curves with a dramatic increase of the TMRh fluorescence in the transition region. The baselines above the main transition are not quite linear; this is probably due to a noticeable conformational change between different configurations of the TMRh−ss-DNA complex in this temperature range (Vámosi et al., 1996). If we determine the baseline on the high-temperature side of this sharp peak, the small hump appears in the extent-of-melting curve. The prominence of this overshoot depends on the baseline chosen, but the T_m is relatively insensitive to this.

The TMRh anisotropy melting curves (Figure 4) can be divided into the same three groups corresponding to the strands that are labeled with TMRh (i.e., TMRh labeling on the h, r, or x strands) as for the TMRh fluorescence intensity melting curves. For the rR molecules, the r (560/590) values display a relatively sharp transition to lower values at the T_m and are a good indicator for the helix−coil transition between 30 and 40 °C. From 40 to 70 °C, the r (590/560) values decrease gradually from 0.09 to 0.05. The melting reaction is also evident from the anisotropy values for the hR and xR samples, but the melting transition is not so evident in the temperature range of 30−40 °C. The r (590/560) values, which decrease gradually from 0.15 to 0.08 in the temperature range of 40−70 °C, are significantly higher for the hR and the xR samples than for the rR samples. This is consistent with the behavior of the TMRh fluorescence intensity described in the previous paragraph.

DISCUSSION

Thermal Denaturation of the Molecules as Observed by Relative and Absolute Changes of the Fluorescence Spectroscopic Parameters. The different spectroscopic signals that we have used to follow the progress of the thermal denaturation of the $3HS_n$ junctions emphasize conformational changes in different parts of the DNA molecule. Nevertheless, all thermodynamic analyses of the fluorescence intensity melting curves give a concordant description of the helix−coil transition of the DNA. The two-state analysis of the extent-of-melting curves of all molecules with and without bulges have the same T_m within 0.5 °C when the melting is monitored by the direct fluorescence intensity of TMRh, by the fluorescein melting curves or by the $(\text{ratio})_A$ values (the concentrations of the branched molecules are chosen to be identical in all experiments). The T_ms are also the same for all different samples (3H as well as $3HS_n$ molecules). The deviations in the wings of the TMRh melting curves (Figure 2) are correlated with the particular arm that is labeled with TMRh, not with the number of nucleotides in the bulges. The extent of these deviations (the most extreme case is shown in Figure 2B) depends on the way the baselines are fitted and the number of data points on either side of the main melting transition that is included in the fit.

The thermodynamic parameters that are derived from the fluorescence intensity melting curves (see Results and Table 1) are also similar for all molecules and are internally consistent throughout the whole series of molecules for each method of analysis. This means that the extent-of-melting curves derived from the fluorescence measurements do not detect a noticeable destabilization of the three-way junction molecules induced by bulged nucleotides at the point of branch exchange. This is true for the extent-of-melting curves derived from the FRET measurements, as well as from the fluorescence intensities.

An Estimate of the Effect of the Loss of Base Stacking at the Branch Point on the Overall ΔH and ΔS *of the Helix−Coil Transition*. The three-way junctions reported in this work are constructed from three strands of single-stranded DNA that possess complete complementarity (except for the bulges) such that the three DNA arms are fully hybridized. We have found by FRET (Stühmeier et al., 1997) and electrophoresis (Welch et al., 1993) studies that the three-way junctions without a bulge used in this study have a trigonal arrangement of the three intact helical arms. This trigonal structure is only possible if the stacking interactions between the end base pairs at the branch point are considerably distorted, if not completely annihilated, compared to the usual base-pair stacking in a continuous helix. This is also consistent with reactivity of thymine bases located at the point of strand exchange toward out-of-plane attack by osmium tetroxide under all conditions (Welch et al., 1993). Assuming that there is no stacking between the end base pairs at the branch point, the extent of base-pair stacking for junctions with no bulged nucleotides would be less than that found in a fully complementary two-stranded duplex with 30 base pairs by four unsatisfied stacking interactions of terminal base pairs (there are six base-pair helix ends in our model of the three-way junction compared to two helical ends in the corresponding helix). This decrease in the extent-of-stacking leads alone to a lower overall expected difference between the enthalpy of the fully base-paired and the fully single-stranded forms for the branched structures compared to the corresponding longer 30 bp nonbranched two-stranded duplex structures. To a first approximation, the additional four helical ends in the branched structure would correspond to a decrease in the stacking interactions of two consecutive base pairs in the middle of a helical duplex. This would decrease the magnitude of the overall ΔH of the duplex strand hybridization by approximately 16 kcal/mol and possibly the magnitude of the ΔS by 50 cal mol^{-1} K^{-1} [using the average thermodynamic values for two base pairs melting

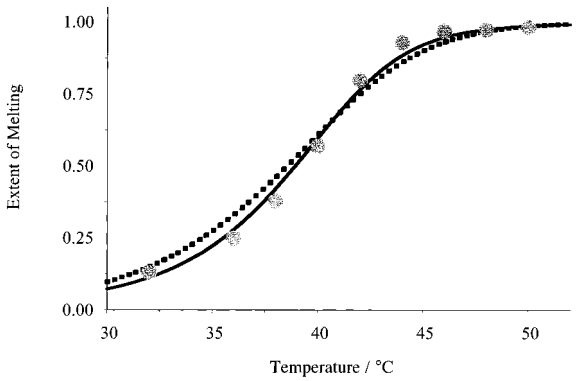

FIGURE 5: Example of the difference between the fit of a two-state fit (dashed curve) and statistical zipper model fit (solid curve) to melting data (open circles) of a fluorescein fluorescence thermal denaturation curve of the 3Hs1(hFxR) sample.

in the middle of a helix[5] (Breslauer et al., 1986)]. Such values of ΔH and ΔS could make significant thermodynamic contributions to the free energy change of a local structural transformation, but the average contribution when considered *per base pair* is only ΔH/bp $\approx$ 0.5 kcal (mol bp)$^{-1}$ and ΔS/bp $\approx$ 0.0015 kcal (mol bp)$^{-1}$ K^{-1}. The accuracy in predicting ΔH/bp and ΔS/bp is not so refined that we can compare the experimentally derived quantities with literature values in order to check the validity of this simple prediction.

Two-State Model Simulations of the Fluorescence Intensity Melting Curves. To a first approximation, it is interesting to compare the stability and thermal denaturation curves to a 30 bp duplex with no branching discontinuities. We would not expect to be able to analyze the melting curves of a simple coaxial 30 bp duplex in terms of a two-state strand dissociation process. In accordance with this expectation, if the assumption is made that the three strands associate as a two-state trimolecular association (i.e., all 30 base pairs simultaneously, see Table 1), then the derived ΔH/bp from the van't Hoff analyses of the fluorescence melting curves is significantly lower than the average values ΔH/bp which have been determined calorimetrically (Breslauer et al., 1986) (see Table 1). In addition, a simulation of the melting curves over the whole temperature range based on a simple two-state analysis of the melting data exhibits consistent deviations from the data (see Figure 5), whereby the slope of the fitted curve in the transition region is less steep than the data or than the fit using the zipper model. *A priori*, one could not say that the branch structure would not melt as a two-state 30 bp melting process; however, our expectations that it does not were borne out by our experiments. Because there are no other variables in the two-state trimolecular model besides the overall ΔH (two-state) and ΔS (two-state) values to parameterize the melting curves, we cannot derive any mechanistic insight from these simulations other than that the three-way junction does not melt in one step as a 30 bp structure as dictated by the two-state model. For similar reasons, we can say that the three-way junction does not melt as a two-state bimolecular 10 bp process corresponding to the length of the arms (see Table 1). On the other hand, the thermodynamic estimates of ΔH/bp and ΔS/bp are closer to those expected from literature values if the transition region of the melting curves are interpreted in terms of a bimolecular, two-state melting of a 20 bp duplex (see Table 1). This is discussed further in the next section.

Zipper Statistical Model Simulations of the Melting Curves. The two-state model assumes that the complete helical structure of the duplex form of the DNA oligomer is not interrupted; that is, intermediate structures with incomplete base stacking are not considered when deriving the thermodynamic and the spectroscopic information from the melting curves. The statistical model lifts the constraint that there are not observable intermediates which is the hallmark of the two-state model, and each of the intermediates contributes singularly to the fluorescence signal at any temperature. A statistical weight is assigned to all possible intermediate structures with different numbers of unpaired bases at the ends of an incompletely base-paired duplex structure. The statistical zipper model provides a way to estimate the length of consecutively stacked base pairs that act cooperatively as a helical unit in the melting process, as well as providing an estimate of which base pairs contribute most to the fluorescence change during the melting process when they become broken.

The statistical zipper model has inherently many parameters; even in its simplest form every base pair can be assigned individual values for its enthalpy and entropy changes when passing from the helix to the coil state. The thermal denaturation curves do not contain nearly enough detail to employ more than a few variable parameters in order to achieve a satisfactory fit to the data. In addition, the baselines cannot always unequivocally be estimated, and the best fit of the statistical model will depend on the choice of baselines. For this reason we have decided to use the same values of ΔH/bp and ΔS/bp for all base pairs. Even with this restriction, when both values of ΔH/bp and ΔS/bp are varied, the shape of the curve, as well as the position of the transition temperature, can be varied considerably, and for comparing simulated melting curves with different length duplexes, it is useful to keep the value of ΔS/bp constant at 0.024 kcal (mol bp)$^{-1}$ K^{-1}, which is a value in the range usually reported from melting studies of small oligonucleotides (Breslauer et al., 1986). Other important fitting variables which have a major influence on the shape of the measured fluorescence melting curve are which base pairs and the number of base pairs that contribute to the fluorescence signal; however, these parameters can be fairly well determined, because the shapes of the melting curves are strongly dependent on the values of these latter variables.

The measured melting temperature and the form of the melting curves for the 10 bp three-way junctions are significantly different from those expected from simulations using the zipper model for a comparable 10 bp duplex with the same complementary sequence as the three-way junction (assuming that ΔS/bp is 0.024 kcal (mol bp)$^{-1}$ K^{-1}). The simulated curves have the same deviations from the data as the two-state fits discussed in the above section (i.e., the transition curves are too shallow). The fits using the zipper model are in general not as satisfactory when using a 30 bp duplex as when using a 20 bp duplex (keeping the ΔS/bp

[5] These values are very approximate and do not take the in-plane interactions between the base pairs into account (such as hydrogen bonding, which is, however, partially compensated by trading water-base for base-base interactions).

[6] Thus, as an example say that the end region that quenches has four base pairs. If all four base pairs are intact, we have maximum quenching; if only the end base pair of the four is broken there is 75% maximum quenching; if two of the end base pairs of the four are broken, the quenching is 50% effective; and so on.

constant at 0.024 kcal (mol bp)$^{-1}$ K^{-1}), although the 30 and 20 bp duplex fits are sometimes indistinguishable considering the error in determining the baselines. The difference between simulated fluorescence melting curves for 20 and 30 bp duplexes (using the zipper model) with fluorescence labels on the end of the helices, is not very large. The fits using a 30 bp duplex model are in general indistinguishable within the error of the measurement from the 20 bp duplex model if the values of ΔH/bp and ΔS/bp for the 30 bp duplex simulation are ~5.7 kcal (mol bp)$^{-1}$ and 0.018 kcal (mol bp)$^{-1}$ K^{-1}. In general, the data for the three-way junction can be represented best by the zipper statistical model of a simple continuous 20 bp duplex (with no branch points), if the values for ΔH/bp and ΔS/bp are close to the average values from the literature (Breslauer et al., 1986); these values of ΔH/bp and ΔS/bp [~7−8 kcal (mol bp)$^{-1}$ and 0.024 kcal (mol bp)$^{-1}$ K^{-1}] that we have used from fitting our data to a simple zipper model using a 20 bp duplex are of course only rough estimates. They serve only as a guide for comparing simple models for the thermally induced dissociation in order to estimate the size of the structural elements that contribute collectively to the overall stability of the three-way junction. These parameters give a good global representation of the melting curves over the entire temperature range. This means that when we use reasonable average thermodynamic parameters per base pair (ΔH/bp and the ΔS/bp) similar to those derived from calorimetry measurements on small defined oligonucleotides (Breslauer et al., 1986), the zipper statistical model accounts well for the shape of the melting curves in Figure 2. This indicates that the consecutive base-pair links inherent in a simple 20 bp two-stranded helix are sufficient to represent the observed cooperativity in the helix−coil transition of the three-way junction with equal arms of 10 base pairs in spite of the disruption in the continuity of the helix at the point of branch exchange. In this respect, it is important to note that the number of base pairs between the free ends of the helical arms of the three-way junction is 20 base pairs and that the continuous strand connecting two arms is also 20 base pairs; thus, it is reasonable from this point of view that the melting data for the three-way junction can be well represented by a simple 20 bp duplex.

Both the statistical zipper model and the two-state model fit the data better when assuming a 20 bp contiguous duplex than when assuming the equivalent duplex to be a 10 or a 30 bp contiguous duplex [assuming that ΔS/bp = 0.024 kcal (mol bp)$^{-1}$ K^{-1} for the statistical zipper model], although the major discrepancy is found when assuming a 10 bp duplex with the zipper model. However, the zipper model always fits the shape of the extent-of-melting curves better than the two-state model, especially in the transition region (Figure 5). This is to be expected due to the large number of base pairs. This is apparent in every curve, no matter which optical parameter is used to follow the transition. This deviation of the two-state model is shown in Figure 5 for a fluorescein intensity melting curve; of all the melting curves, the fluorescein melting curves are better represented by the two-state model than the TMRh melting curves. Interestingly, if *both* ΔH/bp and ΔS/bp are varied in the statistical zipper model, the resulting values of ΔH/bp and ΔS/bp are close to those found for the two-state analyses for every length duplex.

The thermodynamic parameters per base pair required to simulate the melting data with a statistical model for the three-way junctions with and without bulges are very similar; the same is true for the extent-of-melting curves for all the three-way junction samples (with and without bulges). In addition, for all the $3HS_n$ molecules with bulges, the extent-of-melting curves are essentially indistinguishable for each "*n*" regardless of which arm is fluorescently labeled. These data, together with the fact that the melting curves of a three-way junction with 30 complementary base pairs can be simulated well with a duplex model with only 20 base pairs (which is the number of nucleotides between any two ends of the helical arms of the three-way junction) and not by a 10 bp duplex, indicate that the helix−coil melting process proceeds simultaneously and independently from the free ends of the helical arms, and the progression of the helix−coil reaction (the unzippering) proceeds toward the branch point from the ends that are separated by 20 base pairs (additional evidence for this is presented is the next paragraph). The cooperative unit of melting of our three-way junctions with 10 bp arms is about 20 base pairs.

Fluorescence Intensity Changes Are Associated Mainly with a Few Base Pairs at the End of the Helix. The mechanism of unzippering from the ends during the helix−coil transition is evident from the satisfactory representation of the fluorescence melting curves with the statistical mechanical model which incorporates partially melted intermediate states. The fluorescence changes are most sensitive to structural changes at the helical ends (where the dyes are attached), and the simulations show that the form of the experimental fluorescence melting curves can be represented best when the primary intermediate states with nonhelical nucleotides begin at the open ends of the helical arms. The best fit to the data using the zipper model is found when the change of the TMRh and fluorescein fluorescence is limited to the melting of both the second and third base pairs (from the 5′ end) as the helix structure melts from the end of the duplex. The simulations were done such that each separate base pair in the region of the DNA which is selected to interact with the dye contributes an equal fractional amount of quenching.[2] It is clearly seen in the simulations that, if the base pairs are chosen at the end of the helix, the melting curve is too shallow; if too many base pairs are included, the curve is too sharp (especially at the beginning and end of the transition). This is a more realistic representation of the mechanism of melting than the two-state model; the stepwise mechanism of the melting reaction and the local molecular changes that contribute the most to the fluorescence signal are taken into account.

The extent-of-melting curves derived from all TMRh fluorescence melting data for molecules are labeled with TMRh on the r-strand are all fairly symmetrical, as shown in Figure 2A. The TMRh r-strand melting curves show the greatest increase in the TMRh fluorescence upon melting (Figure 3), and the decrease in the fluorescence intensity after the melting transition has taken place is nearly linear. The TMRh x-strand melting curves also show a large increase in the fluorescence upon melting; however, the decrease in the fluorescence intensity following the major transition is nonlinear. The rate of decrease of the TMRh fluorescence becomes less as the temperature increases. If the data above 45−50 °C are included in the baseline fits, then the resulting extent-of-melting curves show the "overshoot" seen in Figure

2C (and to a much less extent in Figure 2B, for the TMRh h-strand melting curves). This probably corresponds to a redistribution between the different configurations of the TMRh−DNA complex as a function of temperature that has been reported for TMRh ss-DNA (Vámosi et al., 1996); this temperature-dependent reaction is apparently more pronounced in this temperature range for the sequences of the TMRh x-strands than for the other two labeled strands. It is another indication [in agreement with our earlier studies (Vámosi et al., 1996)] that the different apparent fluorescence quantum yields of the TMRh ss-DNA is related to the formation of a complex between the TMRh and the DNA strand and not to a simple dynamic quenching phenomenon. For the TMRh h-strand extent-of-melting curves (Figure 2B; this is the labeling vector with the least fluorescence increase following the melting transition), and only slightly apparent in the TMRh h-strand extent-of-melting curves, there is a sloping increase that is not seen in the corresponding curves derived from the other fluorescence parameters. This is probably due to the same phenomenon that is responsible for the overshoot seen above the duplex-melting transition for the melting curves involving the TMRh x- and the TMRh h-strands. The TMRh attached to the single strands that are formed at the beginning of the transition are undergoing a redistribution between the states with different quantum yields simultaneously with the melting transition, and this leads to a nonlinearity in the baseline region for these TMRh-labeled vectors. This nonlinearity can be more or less accented depending on which temperature points are used for the baseline fits; but the congruity between melting data for all the molecules with different sizes of bulges, but with the same TMRh labeling, is not influenced by this effect.

It is important to realize that even though some details of the melting curves depend on the localization of the dye to a particular region of the DNA molecule, the T_m from the fluorescence melting curves is still strongly dependent on the thermodynamics of the whole molecule; the statistical models show explicitly that changes in the occupation of intermediate states, which do not involve fluorescence changes, are still observable by localized fluorescence probes, because at equilibrium all states are interconnected through the equilibrium distribution of states. It should not be assumed that, just because the fluorescence changes are confined to specific locations, these local molecular changes take place independently of concomitant changes in distal regions of the molecule. The degree of coupling is a subtle function of the sequence and of the degree of connectivity of neighboring sequence sections.

A Comparison between the Results of Our Fluorescence Melting Curves and Calorimetric Evidence as to Whether the Presence of a Bulge Destabilizes the Three-Way Junction. Ladbury et al. (1994) have reported an isothermal titration calorimetry study on short-arm three-way junctions with bulges. They first determined an average of the thermodynamic parameters for the three separate arms of the three-way junction. The sum of these one-arm values were then compared to the sum of the average one-arm values plus the average of the total formation of the three-way junctions. The difference between the two cases was attributed to the presence of the bulge. Using their table, we can calculate the following values for the formation of a bulge in the branch point of a three-way junction at 25 °C: $\Delta H = 5$ kcal (mol bulge)$^{-1}$ and $\Delta S = -20$ cal K^{-1} (mol bulge)$^{-1}$. These ΔH and ΔS values are derived from a comparison of three helical arms and the assembled junction; this means that the connection of the three arms at the branch point decreases the overall stability of the duplex structure.

The hypothetical decrease in the ΔH that we have calculated three sections above, considering only losses in stacking interactions at the branch point, actually compares a 30 bp two-stranded duplex with a structure having three separate arms (i.e., six helical ends). This is not the same structure to be compared to the three-way junction in the study by Ladbury et al. (1994) (they compared the stability of the junction to a sum of the three individual arms, i.e. both the three-way junction and the three individual arms have six helical ends). Their calorimetric results show that the expected destabilization of the three-way junction compared to the 30 bp duplex would be even larger than we calculated. If the values of Ladbury (Ladbury et al., 1994) for the destabilization due to the branched junction were distributed over all base pairs of a 20 bp duplex (the statistical model that represents best the melting of our three-way junctions), this would contribute approximately −0.25 kcal mol^{-1} bulge^{-1} and −1 cal K^{-1} bulge^{-1} to the ΔH/bp and ΔS/bp. Such small differences would lie below the error of our simple statistical mechanical analysis; however, if there were a destabilization of our junction molecules as large as reported by Ladbury et al. (1994), we should be able experimentally to detect the difference in the T_m between two junctions that are at the same concentration and are identical except for the presence or the absence of a bulge from the melting curves themselves.

However, we do not observe a destabilization of the junctions due to the presence of a bulge; the T_ms determined from the fluorescence intensity melting curves are identical for all three-way junctions (the concentrations of the junction molecules are identical for the melting experiments). If there were a significant destabilization (or stabilization) of the three-way junction, we would be able to observe this by a lowering (or raising) of the T_m.

Possible Explanations Why the Spectroscopic Characteristics of Different Single-Stranded TMRh-Labeled Oligonucleotides Differ at Higher Temperatures. The relative increase in the TMRh fluorescence intensity from the beginning to the end of the melting transition depends strongly on which arm is labeled (Figure 3). The quantum yields of TMRh when attached to the duplex DNA helices below their melting temperature are very similar for all arms of the intact three-way junction (see Results). However, the apparent quantum yield of the TMRh molecules covalently attached to single-stranded DNA above the melting transition are different for the different labeling vectors. The differences between the molecules labeled on the H, R, and X arms are noticeable also in the extent-of-melting curves derived from the corresponding TMRh fluorescence melting curves (Figure 2). We suggest at least two possibilities for this behavior.

(1) One possibility is that the apparent quantum yield of TMRh could be influenced by the formation of hairpins above the major ds- and ss-strand transition. For the following discussion, we make the constraint that only hairpins where more than one consecutive base is involved in base pairing have to be considered. Inspection of the sequences shows that hairpins can be proposed for all three strands (Figure 6). If these hairpins are stable above

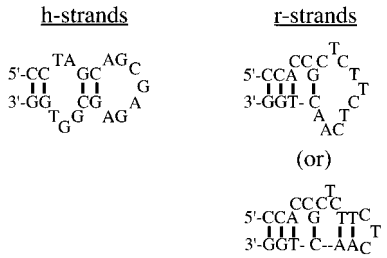

FIGURE 6: Possible hairpins that could form with the different single strands. The x-strand cannot form a stable hairpin structure; however, stable hairpins can be formulated for the h-strands (left) and the r-strands (right). Base pairing is indicated by vertical lines.

temperatures where the corresponding multistrand structures no longer exist, the ds structure at the open end of the hairpins would likely quench the fluorescence, because the apparent quantum yield of TMRh is in general considerably lower for the ds-TMRh−DNA complex than for the ss-TMRh−DNA complex at any particular temperature (Vámosi et al., 1996). Oligonucleotides similar to those here form hairpins and are stable at temperatures above 40 °C; the apparent quantum yields are lower than the pure single-stranded molecules, but higher than the pure double-stranded structures (G. Vámosi et al. unpublished results). Only a hairpin with two GC base pairs at the end can be formed by the x-strand oligonucleotide. The relatively high apparent quantum yield of the x-strand (compared to the other strands) at the end of the duplex-single-stranded transition indicates that hairpin structures, which would lead to a reduced apparent quantum yield of the TMRh (Vámosi et al., 1996) do not exist for this oligonucleotide at higher temperatures.

Hairpins with more than just two base pairs at the $(CG)_2$ ends can be formed for both the h- and r-strands (Figure 6); however, the fluorescence melting curves for the corresponding three-way junctions where these strands are labeled with TMRh are very different. If the difference in the melting curves of the molecules with labeled h- and r-strands were to be attributed only to hairpin formation with a helical stem at the end, we would not expect such a large difference in these two vectors. On the other hand, we would also not expect the relative fluorescence intensity right above the T_m to be similar for those molecules with TMRh on the r- and x-strand (the x-strand cannot form an extended hairpin that is stable at this temperature); nevertheless, this is the case (see Figure 3). This is an argument against interpreting the different forms of the melting curves in terms of only hairpin formation; however, further experiments on single-stranded labeled molecules with different sequences are necessary to answer this question.

(2) The second possibility concerns the nucleotide sequence at the 5′ ends where the TMRh is conjugated [Figure 1 of Stühmeier et al. (1997)]. The first two nucleotides in the sequence at the 5′ ends are the same for all labeled strands (5′-CC). The first four nucleotides in the end sequence, in order of increasing quenching capacity, are 5′-CCAC (r-strand), 5′-CCAG (x-strand), and 5′-CCTA (h-strand). The extent of quenching may be influenced especially by the third nucleotide from the 5′ end. The TMRh of the h-strand is considerably more quenched than for the two other strands, indicating that thymine, in the third position, may be involved in the effective quenching of the TMRh fluorescence.

The proposed role of thymine as an effecitve (even if only possibly an auxiliary) participant in the quenching process of the TMRh fluorescence is supported by a comparison of the shape of the fluorescence intensity melting curves. The fluorescence intensities of the xR and rR molecules are not as strongly quenched at the end of the melting process (at 42 °C) as the hR molecules. At temperatures above the thermal denaturation (higher than), the xR molecules undergo a more rapid transition from a lower to a higher quenched form (Figure 3) than the rR molecules. The x-strand has two thymine residues positioned five and six bases away from the 5′ end. These thymines could become accessible to the TMRh at the high-temperature end of the transition due to increased thermal motion of the molecules, and this could lead to increased quenching compared to the r-strand; the r-strand has no thymines within eight nucleotides from the 5′ end.

If the results and interpretations of (Seidel et al., 1996) concerning the fluorescence quenching of several coumarin dyes by a single mononucleotide can be extrapolated to tetramethylrhodamine (unpublished results using rhodamine 6G show similar behavior to the coumarins; C. Seidel, personal communication), we might expect to find a correlation of the extent of quenching (by photoinduced electron transfer) with distance of the first guanine in the oligomer from the dye molecule attached to the 5′ end. We do not find this correlation, but it is difficult to compare their results on coumarins interacting with mononucleotides (the dye and nucleotide molecules are either free in solution, or the dye molecules are covalently bound to the mononucleotides) with our results where TMRh is bound to an oligomer with an extended heterogeneous sequence.

We have shown recently that TMRh covalently attached to the 5′ end of double- and single-stranded oligomers of DNA can form separate, well-defined distinct complexes with the nucleic acid strands (Vámosi et al., 1996). The strong temperature dependence of the apparent fluorescence quantum yield is due to a redistribution of the TMRh molecule, that is covalently labeled to the 5′ end of DNA, among three different states of complexation on the DNA molecule, where each state has distinct and disparate fluorescence properties. It is conceivable that the sequences of the DNA at the 5′ end plays a major role in defining the distribution of the TMRh molecule among the different TMRh−DNA complex configurations and thereby influences the effective apparent quantum yield and anisotropy of the covalently attached TMRh on single-stranded DNA. Thus, even though we have noted an apparent correlation of the fluorescence intensity and anisotropy of TMRh−DNA(ss) complexes with the sequence distance between the dye and thymines, this does not mean that the thymine is the actual molecular quencher. Further experiments must be done to clarify the role of the DNA sequence on the apparent quantum yield of TMRh.

CONCLUSIONS

The thermal stability of all the three-way molecules (determined by observing the fluorescence signals) do not exhibit a dependence on the presence, or the size, of the bulge. Simulations of the melting curves with a statistical model corresponding to simple duplex molecules indicate that the important dimension (cooperative length) of the DNA structure controlling the progress of the melting of the junction seems to be the distance between the ends of neighboring helical arms. The disruption of the helical

structure during thermal denaturation appears to proceed from the free outside ends of the helical arms and proceed in a zipper fashion toward the branch point. A sequence dependence of the fluorescence intensity and anisotropy of TMRh attached to the 5′ end of single-stranded oligomers could be surmised from the melting curves.

ACKNOWLEDGMENT

F.S. and R.M.C. thank G. Vámosi and C. Gohlke for communications of their data prior to publication and many valuable discussions of O. Holub and A. Zechel for reading the manuscript.

APPENDIX

The Statistical Mechanics Zipper Model. The statistical weights of the different conformations can be described as follows [see Poland and Scheraga (1970) for a general overview]. The number of base pairs in the coil state on the left and right ends of an N bp duplex are defined as l and r. The probability that any base pair exists in the helix or coil state can be calculated using the following partition function:

$$Q = \sum_{\{N-r-l>0\}} \prod_{i=l+1}^{i=N-r} s_i \qquad \text{(A1)}$$

The statistical weights s_i (which are functions of temperature) are defined as

$$s_i(T) = \exp[-\Delta G_i/RT] = \exp[-(\Delta H_i - \Delta S_i T)/RT] \qquad \text{(A2)}$$

ΔG_i is the change in the free energy passing from the coil to the helix state for the ith base pair ($i = 0$ is defined as the left end of the sequences). ΔH_i and ΔS_i are the corresponding changes in enthalpy and entropy in passing from the coil to the helix state. ΔH_i and ΔS_i values are assumed to be independent of temperature. The statistical weight of the coil state for every base pair is defined to be 1. The constraints over which the variables r and l can vary are defined by the set of numbers $\{N - r - l > 0\}$; that is, every product term is comprised of components (s_i values) where i varies from $l + 1$ to $N - r$. The sum of these product terms extends over all possible variations of r and l such that $\{N - r - l > 0\}$. These products and sums are carried out numerically using vectors of s_i values, calculated from the ΔH_i and ΔS_i values at every temperature (the vectors are N long at every temperature).

The fraction of all Lth base pairs existing in the helix state at temperature T is

$$f_L^h(T) = \sum_{\left\{\substack{N-r-l>0 \\ l<L}\right\}} \prod_{i=l+1}^{i=N-n} s_i/Q \qquad \text{(A3)}$$

In eq A3, the constraints on the set of valid r and l values have been extended compared to those in eq A1 to include the condition $l < L$. The condition $l < L$ must be true, otherwise the Lth base pair would not be in the helix state. These calculations can be carried out numerically easily and rapidly in a computer.

The fluorescence at every temperature is calculated relative to the fluorescence of the complete coil state at every temperature. We define $F_h^L(T)$ to be the fluorescence change when the Lth base pair passes from the helix to the coil state [in general $F_h^L(T)$ is a function of the temperature]. The total measured fluorescence change at any temperature (at any position within the melting curve) is equal to the sum of the separate fluorescence contributions for each individual base pair (which is proportional to the fraction of each base pair in the helix state):

$$F_{\text{total}}(T) = \sum_{L=1}^{L=N} F_h^L(T) f_L^h(T) \qquad \text{(A4)}$$

$F_h^L(T)$ depends on L, and only the base pairs near the position of labeling are expected to contribute significantly to the fluorescence change when passing from the helix to the coil state. The values that are varied in the simulations are ΔH_i, ΔS_i, and the values of $F_h^L(T)$. The normalized value of $F_h^L(T)$ is calculated for the temperatures of the melting curves, and the variance between the fit and the data is minimized in an iterative process.

The All-or-None Model for the Dissociation of Duplexes. The dissociation of a duplex to two single strands is described by the van't Hoff equation for a bimolecular process:

$$K_d(T) = \frac{[ss_1][ss_2]}{[ds]} = \frac{c_0\alpha^2}{1-\alpha} = \exp\left(-\frac{\Delta H}{RT} + \frac{\Delta S}{R}\right) \qquad \text{(A5)}$$

We define

$$A(T) = \frac{K_d(T)}{c_0} = \frac{\alpha^2}{1-\alpha} \qquad \text{(A6)}$$

so that

$$\alpha(T) = \frac{-A(T) + \sqrt{A(T)^2 + 4A(T)}}{2} \qquad \text{(A7)}$$

where K_d is the dissociation constant, [ss_1], [ss_2], and [ds] are the concentrations of the single- and double-stranded molecules, c_0 is the duplex concentration if all the molecules are in the duplex form, α is the molar fraction of single strands (or the extent-of-melting), ΔH and ΔS are the molar enthalpy and entropy change of the two-state transition, R is the gas constant, and T is the temperature in kelvin.

$\alpha(T)$, which varies from 0 to 1, is fit to the data for which the baselines have been extracted by straight lines (reference).

The data can also be fit directly to the data by fitting $\alpha(T)$ together with the straight lines for the lower and upper baselines; in this case the expression is

$$\text{Fluorescence} = a_1 + b_1 T + \alpha(T)\{(a_2 - a_1) + (b_2 - b_1)T\} \qquad \text{(A8)}$$

a_1, b_1, a_2, and b_2, are the straight-line parameters for the lower and upper baseline fluorescence values; the temperature dependence of the baselines is assumed to be a straight line.

REFERENCES

Breslauer, K. J., Frank, R., Blöcker, H., & Marky, L. A. (1986) *Proc. Natl. Acad. Sci. U.S.A. 83*, 3746−3750.
Clegg, R. M. (1992) *Methods Enzymol. 211*, 353−388.

Clegg, R. M., Murchie, A. I. H., & Lilley, D. M. J. (1994) *Biophys. J. 66*, 99−109.
Husler, P. L., & Klump, H. H. (1994) *Arch. Biochem. Biophys. 313*, 29−38.
Husler, P. L., & Klump, H. H. (1995) *Arch. Biochem. Biophys. 322*, 149−166.
Ladbury, J. E., Sturtevant, J. M., & Leontis, N. B. (1994) *Biochemistry 33*, 6828−6833.
Leontis, N. B., Kwok, W., & Newman, J. S. (1991) *Nucleic Acids Res. 19*, 759−766.
Lilley, D. M. J., Clegg, R. M., Diekmann, S., Seeman, N. C., Kitzing, E. v., & Hagerman, P. M. (1995) *Eur. J. Biochem. 239*, 1−2.
Marky, L. A., & Breslauer, K. J. (1987) *Biopolymers 26*, 1600−1620.
Overmars, F. J. J., Pikkemaat, J. A., Elst, H. v. d., Boom, J. H. v., & Altona, C. (1996) *J. Mol. Biol. 255*, 702−713.
Poland, D., & Scheraga, H. A. (1970) *Theory of Helic-Coil Transitions in Biopolymers*, Academic Press, New York.
Seidel, C. A. M., Schulz, A., & Sauer, H. M. (1996) *J. Phys. Chem. 100*, 5541−5553.
Stühmeier, F., Welch, J. B., Murchie, A. I. H., Lilley, D. M. J., & Clegg, R. M. (1997) *Biochemistry 36*, 13530−13538.
Vámosi, G., Gohlke, C., & Clegg, R. M. (1996) *Biophys. J. 71*, 972−994.
Welch, J. B., Duckett, D. R., & Lilley, D. M. J. (1993) *Nucleic Acids Res. 21*, 4548−4555.
Welch, J. B., Walter, F., & Lilley, D. M. J. (1995) *J. Mol. Biol. 251*, 507−519.
Zhong, M., & Kallenbach, N. R. (1993) *J. Mol. Biol. 230*, 766−778.
Zhong, M., Rashes, M. S., & Kallenbach, N. R. (1993) *Biochemistry 32*, 6898−6907.
Zhong, M., Rashes, M. S., Leontis, N. B., & Kallenbach, N. R. (1994) *Biochemistry 33*, 3660−3667.

BI970245X